16

Electron Crystallography of Membrane Proteins

Hui-Ting Chou, James E. Evans, and Henning Stahlberg

Summary

Electron crystallography studies the structure of two-dimensional crystals of membrane proteins or other crystalline arrays. This method has been used to determine the atomic structures of six membrane proteins and tubulin, as well as several other structures at a slightly lower resolution, where secondary structure motifs could be identified. To preserve the high-resolution structure of 2D crystals, the meticulous sample preparation for electron crystallography is of outmost importance. Charge-induced specimen drift and lack of specimen flatness can severely affect the resolution of images for tilted samples. However, sample preparations that sandwich the two-dimensional crystals between symmetrical carbon films reduce the charge-induced specimen drift, and the flatness of the preparations can be optimized by the choice of the grid material and the preparation protocol. Data collection in the cryoelectron microscope using either the imaging or the electron diffraction mode has to be performed after low-dose procedures. Spot scanning further reduces the charge-induced specimen drift.

Key Words: 2D membrane protein crystals; back-injection; sandwich method; spot-scanning; carbon flatness; low-dose; cryoelectron microscopy.

1. Introduction

Structural biology of membrane proteins is of central importance for cellular biology and for the development of new drugs. Membrane proteins represent the majority of today's drug targets in pharmaceutical research. Nevertheless, our databases contain less than 50 unique folds of membrane proteins as compared with several thousand for soluble proteins. Electron crystallography studies the structure of membrane proteins in a two-dimensional crystalline arrangement in a phospholipid bilayer membrane. The atomic models of tubulin *(1)* and of the membrane proteins BR *(2)*, LHCII *(3)*, AQP1 *(4,5)*, the C-ring of Na^+ ATPases *(6)*, nAChR *(7)*, and AQP0 *(8)* were determined by electron crystallography. Several other membrane proteins classified as transporters, ion pumps, receptors

From: *Methods in Molecular Biology, vol. 369*
Electron Microscopy: Methods and Protocols, Second Edition
Edited by: J. Kuo © Humana Press Inc., Totowa, NJ

and membrane bound enzymes have been studied at slightly lower resolution allowing the localization of secondary structure motifs such as transmembrane helices, and are likely to produce atomic models in the near future (e.g., Hirai et al. *[9]*).

Electron crystallography can be used to study membrane protein structures at resolutions of 3 Å or better (e.g., *[8,10,11]*), demonstrating the value of this approach. Electron crystallography represents an alternative method for structure determination, when fragile membrane protein complexes cannot be grown into three-dimensional (3D) protein crystals for X-ray diffraction or are not available in sufficient amounts for NMR measurements. Membrane-inserting proteins that undergo conformational changes between the soluble and the membrane-inserted state are likely to be best studied by electron crystallography. Two-dimensional (2D) membrane crystals are frequently grown easier than 3D crystals of membrane proteins and offer to the membrane proteins a more native environment than most 3D crystal forms. Membrane crystals also are advantageous for the structure determination of co-crystals, when preformed crystals are to be incubated with protein binding partners.

Technological advancements like the availability of coherent intermediate voltage electron sources and helium-cooled and stable sample stages *(12)* allow the recording of high-resolution data of biological macromolecules. Improvement in CCD camera sizes and recording bit depth allow efficient data recording of electron diffraction pattern *(13)*. In addition, recent advancements in sample preparation with the sandwich-back-injection technique using non-wrinkled carbon films *(14–16)*, and the spot scanning data collection method *(17)* strongly reduce the resolution-limiting charge effect during data acquisition of tilted samples.

2D membrane protein crystallization usually requires detergent-solubilized and purified protein typically at a concentration of 1 mg/mL. Crystallization can be achieved by various methods *(18–22)*. Although the approach that has so far yielded the best-ordered crystals involves slow and controlled detergent dialysis in the presence of added phospholipids *(19)*, there is no one method or condition that is optimized for all proteins.

1.1. Sample Preparation

Sample preparation is as important as the operation of the electron microscope for the recording of high-resolution data of 2D crystal samples. The 2D crystalline arrangement of the sample allows efficient extraction of the structure's signal from extremely noisy images by computer processing. For the choice of the sample preparation, preference is therefore given to methods that perfectly preserve the high-resolution order of the 2D crystals, while the contrast of the preparation is of minor importance.

Cryoelectron microscopy (cryo-EM) grids of 2D crystal samples can be prepared using holey or continuous carbon film support grids. However, holey carbon film grids embed the samples in viscous (liquid) vitrified ice, which in most cases provides inferior electrical conductivity, physical stability, and sample flatness than a continuous carbon film support *(23)*. Grids for cryo-EM imaging of 2D crystals therefore usually employ continuous carbon film support. The following protocol describes the preparation of such grids.

2. Materials

1. Carbon evaporator (should have an oil-free high vacuum).
2. Mica sheets.
3. Petri dishes.
4. Anticapillary self-closing tweezers.
5. Molybdenum transmission electron microscopy (TEM) grids (e.g., 300 mesh Mo grids from Pacific Grid-Tech, TX; see also *[16]*).
6. Humid chamber (home-made, constructed from Petri dishes).
7. Filter paper (Whatman, #1).
8. Liquid nitrogen in a Styrofoam cup, covered with aluminum foil to reduce boiling, for freezing of the sugar embedded grids.
9. For plunge freezing: A plunge freezer, if possible with a closed humid chamber (e.g., the Vitrobot, *see* www.vitrobot.com; or a homebuilt device, *see* **Fig. 1**).
10. For the sandwich method: 4-mm diameter platinum wire loop (available for example from Ted Pella, Inc., Redding, CA).

3. Methods

3.1. Plunge Freezing

2D crystals can be adsorbed to glow-discharged carbon-coated grids, blotted and plunge frozen in ethane slush, cooled by liquid nitrogen (*see* **Fig. 1**), similar to the preparation of cryo-EM grids with the holey carbon film method.

1. Evaporate carbon onto freshly cleaved mica (*see* **Note 1**).
2. Place mica with evaporated carbon into a humid chamber over night, to increase ease in floating the carbon off the mica.
3. Float carbon off the mica onto the surface of a buffer solution. This piece of carbon should be slightly larger than a TEM grid.
4. Pickup the carbon with a TEM grid (*see* **Note 2**).
5. Turn the tweezers with the grid upside down.
6. Remove a part of the liquid on the grid with a pipet.
7. Add 1 to 3 μL of 2D crystal solution (through the grid bars; *see* **Note 3**).
8. Place the tweezers into a plunger (Guillotine).
9. Blot the grid with a filter paper and plunge-freeze in ethane slush (*see* **Note 4**).
10. Transfer the grid into a cryo-holder and image with minimal-dose cryo-EM techniques.

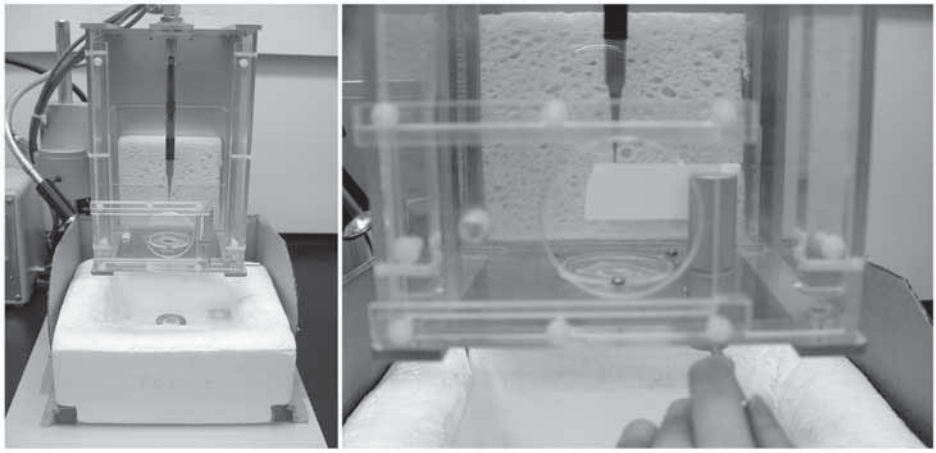

Fig. 1. The plunge-freezing device with a humid chamber. The grid is held by a tweezers in the center of the device (left). The sponge behind the tweezers can be soaked in warm water to increase the air humidity. Samples can be added through the sliding door in front of the tweezers. Blotting for elongated periods of time can be performed with the closed chamber from the outside by rotating the lever manually so that the filter paper blots the sample (right). The tweezers and the tweezers' holding arm is slim, so that plunging of the sample into the LN_2-cooled ethane slush below the chamber can be done without prior removing of the blotting paper.

3.2. Sugar Embedding

Drying of membrane protein crystals in the presence of sugars such as tannic acid ***(3)***, trehalose ***(1,4,24)***, or glucose ***(10)*** can preserve the intact ultrastructure of the proteins, while eliminating the need for quick-freezing.

1. Evaporate carbon onto freshly cleaved mica (*see* **Note 1**).
2. Place mica with evaporated carbon into humid chamber over night, to increase ease in floating the carbon off the mica.
3. Float carbon off the mica onto the surface of a buffer solution.
4. Pickup the carbon with a TEM grid (*see* **Notes 2** and **5**).
5. Place the grid with the carbon film facing up onto three drops of sugar solution (*see* **Fig. 2B** and also **Notes 6** and **7**).
6. Turn the tweezers with the grid upside down. The carbon film is now on the lower side of a hanging drop of sugar under the grid.
7. Remove a part of the liquid on the grid with a pipet (from the top through the grid bars).
8. Add 1 to 3 μL of 2D crystal solution (1 mg/mL) through the grid bars (*see* **Note 3**).
9. Place grid in tweezers for 60 s into a humid chamber, which can be constructed from three plastic Petri dishes (design by Dr. T. Braun, *see* **Fig. 2D**).

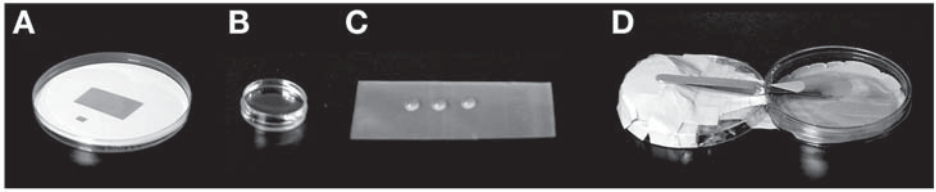

Fig. 2. Sugar embedding of two-dimensional crystals requires a piece of carbon the size of a grid. This carbon can be cut from mica with evaporated carbon **(A)**. The carbon is floated onto a water surface **(B)** and placed onto three drops of sugar containing buffer solution **(C)**. After adding the crystal solution, the grid is allowed to rest for a few minutes in a humid atmosphere that can be created using Petri dishes **(D)**. The edge of the cover of the right Petri dish was broken off over a stretch of 2 cm, forming a hole where the tip of the tweezers can enter. The bottom of the right Petri dish is covered with a wet filter paper, which increases air humidity when the Petri dish is closed.

10. With a pipet, take excess solution off the grid, leaving approx. 1 μL on the grid.
11. Turn the tweezers again upside down, and place the grid flat onto two layers of filter paper with the carbon film facing up.
12. After sufficient blotting time (e.g., 20 s), and potential freezing in liquid nitrogen, observe the grid in the TEM (*see* **Note 7**).

3.3. The Sandwich Method

The sandwich sample preparation method embeds the 2D crystals between two layers of carbon film. This preparation offers two conductive surfaces around the sample, which may help reduce specimen charging and presents a symmetrical charge situation to the electron beam. It may thereby increase the image stability under the electron beam. Another advantage of this method arises when it is used in conjunction with a staining solution, since it can provide a more even staining of the two sample surfaces, even though the second carbon film adds noise to the image (e.g., Golas et al. ***[25]***). The carbon sandwich can be made by placing both carbon films on the same surface of the TEM grid, resulting in the order grid → carbon → sample → carbon ***(25,26)***. Alternatively, the two carbon films can cover both sides of the TEM grid, as described in ***(15)***, resulting in the order carbon → grid/sample → carbon. The latter is presented here:

Perform **steps 1** through **8** as in **Subheading 3.2.** for sugar embedding.

9. Float a second piece of carbon film onto buffer solution (*see* **Note 8**).
10. Lift the carbon film up with a 4 mm diameter platinum wire loop and place it onto the grid from the top side, so that the grid and 2D crystals are sandwiched between the two carbon films (*see* **Fig. 3**).

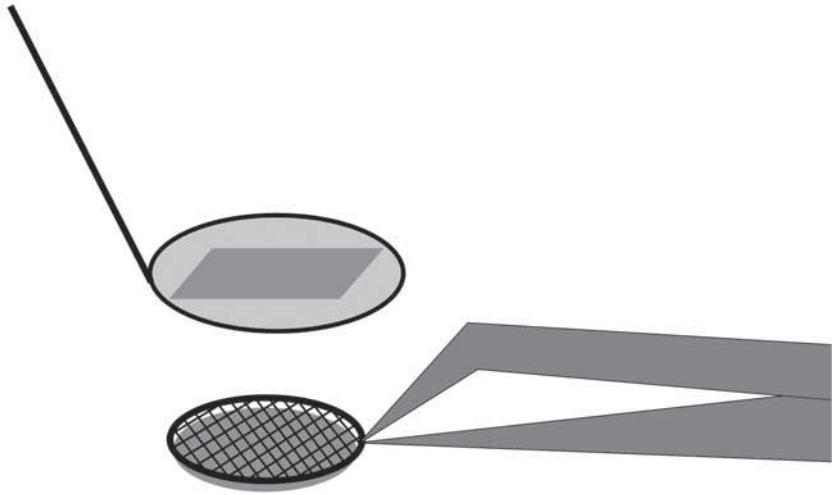

Fig. 3. Transfer of the second carbon film onto the grid to form the carbon film sandwich.

11. Blot the sandwich construction from the edge of the grid, using a piece of torn filter paper.
12. Plunge the grid into liquid nitrogen and transfer into the cryo-EM.

3.4. Electron Microscope Operation

Data collection on the TEM from 2D crystals can be performed by recording images or electron diffraction pattern. Although the Fourier transformations of the images contain amplitudes *and* phases of the sample structure, electron diffraction pattern allow a more reliable determination of the amplitudes but lack the phase information.

3.4.1. Recording of Images

Images are preferably recorded on photographic film and subsequently digitized with a high-resolution scanner, because the current image processing methods benefit from large and coherently connected single crystal images, and the current generation of CCD cameras does not yet offer for higher acceleration voltages (200 kV and higher) a better transfer function at high resolution than the conventional Kodak SO 163 film *(27)*.

Recording of images of 2D crystals requires operation of the electron microscope under low-dose conditions, in which the microscope offers so-called "search," "focus," and "photo" positions. Chose a second condenser aperture of 100 μm or smaller and an objective aperture of 100 μm or larger. Align the TEM in the "photo" position, then setup the "focus" position, and finally the "search"

position. Cycle through the modes exclusively in the order "search" → "focus" → "photo", to prevent hysteresis effects that may make you loose the alignment.

1. Search position: The "search" position uses the defocused electron diffraction mode. Suitable 2D crystal samples are identified at very low illumination intensity, which is best done by using the strong contrast of the shadow image obtained when operating the instrument in over-focused diffraction mode. Use an electron diffraction camera length of 1 m or longer. Set the second condenser lens to strong overfocus to spread the illumination over a large sample area. Set the intermediate lens to overfocus to create a strongly contrasted "shadow image" of the sample. Use a combination of image shift and beam tilt to align the center of the "search" position with the "photo position."
2. Focus position: The "focus" and the "photo" position use the image mode of the electron microscope. In the "focus" position the instrument is operated under identical lens settings as used for the "photo" position, but with additional beam- and image-shift, so that focusing the objective lens can be done adjacent to the sample location of interest. Align first the "photo" position, then copy those settings to the "focus" position, and finally add sufficient beam- and image-shift so that the beam in the "focus" position does not illuminate the sample area of the "photo" position. At 50 kx magnification, this usually corresponds to 3.5-μm beam deflection.
3. Photo position: Images are recorded with the settings of the "photo" position (e.g., 50 kx magnification, 0.5 seconds exposure time on a FEG instrument). Recorded images are modulated by the microscope's contrast transfer function, which can be corrected computationally. To reduce the number of Thon rings, try to work at lower defocus values, if the crystal quality is good enough. When images of tilted samples are recorded, a resolution loss in the direction perpendicular to the tilt axis can frequently be observed, resulting from charge-induced specimen drift and vibration of the sample. Images recorded on photographic film are best inspected by optical diffraction ***(28)*** before digitization.
4. Spot-scanning: When recording images of highly tilted samples, the resolution perpendicular to the tilt axis can be severely affected by charge-induced specimen drift during the acquisition: The illuminated sample area can accumulate electrical charge during the exposure, which gradually deflects electrons into the direction perpendicular to the tilt axis. This effect can be minimized by the sandwich sample preparation method but also by using the so-called s*pot-canning* illumination method ***(17)***: The electron beam on the sample is concentrated into an area of 50 to 100 nm diameter, and step-wise scanned over the sample area, whereas the entire hexagonally arranged spot-scan pattern is recorded onto the same photographic film (*see* **Fig. 4** ***[29]***). Each *spot-scanning* spot has an exposure time of for example 50 ms (when using a FEG instrument), whereas the camera shutter remains open for a few minutes to record the entire *spot-scanning* pattern on one photographic film. Attention has to be paid to adjusting the illumination conditions so that a sufficiently small illumination opening angle is maintained also in the *spot-scanning* mode.

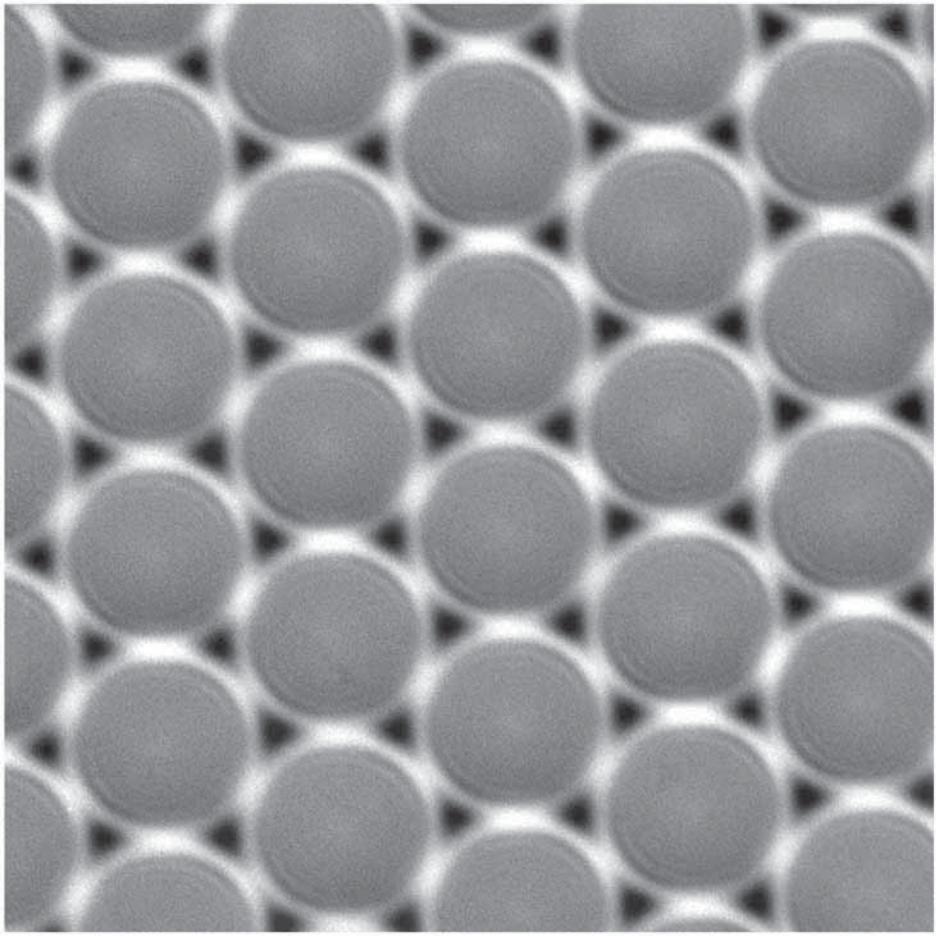

Fig. 4. A micrograph recorded by spot scanning of AQP2 2D crystals *(37)*. The approx. 100 nm diameter spots cover in a hexagonal pattern the micrograph, which in total spans an area of approx. 0.6 μm^2 (dimensions on the sample level). The finer AQP2 2D crystal lattice is not recognizable in the unprocessed image. Such an image can be computer processed to mask the nonexposed dark triangles and the double-exposed bright contact edges between the spot-scan spots, and replace these regions with the average gray value.

3.4.2. Recording of Electron Diffraction Pattern

Electron diffraction pattern are not affected by the contrast transfer function, nor suffer from specimen vibration or drift, and have only very limited dependence on specimen charging during the exposure. Although electron diffraction usually requires well-ordered 2D crystal samples of more than a micrometer in diameter, its recording can be a time-efficient way to obtain a high-resolution

amplitude dataset from tilted samples ***(30)***. Electron diffraction pattern are best recorded on a digital CCD camera, where the superior dynamic range (typically 12 to 16 bit) allows capturing intense low-resolution and weak high-resolution diffraction spots in a single exposure at good signal-to-noise ratio ***(13)***. Depending on the unit cell spacing of the 2D crystal and the expected resolution in a diffraction pattern, a CCD camera of 2048 × 2048 or higher pixel number is required, to sufficiently resolve individual diffraction spots in a diffraction pattern ***(13)***.

To record diffraction patterns, all positions of the low-dose system are setup in diffraction mode. Chose a small second condenser aperture of 10 or 20 μm in diameter, and remove the objective aperture.

1. Search position: The "search" position is set-up as described previously, using the "shadow" image of the overfocused diffraction mode with an over-focused second condenser lens and overfocused intermediate lens.
2. Focus position: The use of this position is optional and may not be required, if the microscope is sufficiently stable, because the electron diffraction focus does not depend on the sample position or sample height. The "focus" position is a copy of the "photo" position and therefore also uses the electron diffraction mode. Focusing is performed *on* the sample. The "focus" mode does not use additional beam or image shift. The alignments of the "photo" and the "focus" mode only differ in the illumination system: A highly excited first condenser lens in the "focus" position is used to dim the sample illumination to the lowest possible intensity. The second (and/or third) condenser lens is then adjusted to again achieve parallel illumination onto the sample. Focusing the diffraction pattern with the intermediate lens can then be done by focusing the *direct* (zero-order) beam on the screen. The focusing settings from the "focus" position are only valid for the "photo" position, if both "focus" and "photo" positions are using the identical parallel illumination conditions onto the sample, which can be verified by checking if the objective aperture border appears sharp in both modes. (This requires the objective aperture to be aligned to the correct height, which is the back-focal plane of the objective lens. Don't forget to remove the objective aperture from the beam for recording the diffraction pattern).
3. Photo position: In the "photo" position, the diffraction pattern of the crystal sample is recorded, using a long exposure time (e.g., 30 s or longer). This position has to provide an alignment with parallel illumination of the sample. Recording of electron diffraction pattern can be done with or without a "selected area diffraction" aperture. If you chose to limit the electrons that contribute to the diffraction pattern using a selected area diffraction aperture, you can illuminate a sample area somewhat larger than the diffracting crystal, allowing a more coherent and homogeneous illumination of the crystal.

The dose for recording one image should be in the order of 500 electrons/nm^2 at liquid nitrogen temperature but can be as high as 2000 electrons/nm^2 at

liquid helium temperature, when information in the resolution range beyond 4 Å is to be recorded. Recent observations of changes in electrical conductivity, viscosity and density of vitreous ice at liquid helium temperatures *(31,32)* might not apply to phospholipid bilayers and/or sugar-embedded samples, which would explain why for 2D crystal samples the usage of helium-cooled instruments has proven strongly beneficial *(33)*.

4. Notes

1. The flatness of the supporting carbon film is of high importance when attempting to record images at high resolution. It is especially important when images of tilted 2D crystal samples are to be recorded because small tilt-angle variations will strongly affect the resolution perpendicular to the tilt axis *(14)*. Uneven or rough carbon film can perturb the specimen flatness, which also can be severely affected by so-called cryo-crinkling of the carbon film *(15,34)* because of different thermal expansion coefficients between the sample and the support grid. Carbon film usually is prepared by carbon evaporation onto freshly cleaved mica, which should be performed at a vacuum better than 5×10^{-6} mbar. Care should be taken that only carbon films from evaporation processes without sparking are used. Carbon films prepared in this way will be smoother on the mica-facing side than on the carbon source-facing side *(35)*. Therefore, the 2D crystal samples should be adsorbed onto the side of the carbon film, which previously was facing the mica.
2. Carbon film should be floated onto the darker, less shiny side of the TEM support grid, which will attach better to the carbon film and result in smoother films *(16)*. Cryocrinkling can be reduced significantly by using grid materials with thermal expansion coefficients similar to that of the sample: Cryocrinkling is strongest with copper, less with titanium, and best with molybdenum grids *(14,36)*. The costly molybdenum grids can be reused after ultrasound cleaning in ethanol. Carbon film will rupture less often when using grids with thicker metal bars, but the visible sample area on tilted grids will be smaller, and the amount of cryocrinkling will increase *(16)*. For high-resolution imaging, 300 mesh molybdenum grids are recommended.
3. The spreading of 2D crystals onto the carbon film can be facilitated by the addition of small amounts of detergents. Bacitracin (0.25 mg/mL) in the sugar solution can, for example, be used as wetting agent to help increase spreading *(37)*. In addition, a pipet can be used to take up a part of the sample/sugar solution at the edge of the grid, and readmit it to the center of the grid several times, to physically increase spreading of the crystals onto the carbon film. Spreading also can improve if longer adsorption times are allowed. This requires the availability of a humidity chamber to prevent sample evaporation during the adsorption time of a few minutes.
4. The sample solution does not evaporate as fast on a closed carbon film as it would do on holey carbon film, allowing longer blotting times. Although the electrical charging of ice contamination on the grid is more difficult to control with this method, vitrification by plunge freezing of 2D crystals on a continuous carbon

film may be preferred over sugar embedding, when a good contrast of undisturbed protein surface structures is required.

5. This method is best done by holding the grid with a self-closing inverted anti-capillary tweezers.
6. The grid is placed for a few seconds onto three drops of buffer solution containing 1 to 7% (w/v) of sugar (e.g., trehalose, glucose, tannic acid), in order to replace the water under the carbon film with the sugar solution (*see* **Fig. 2C**). To maintain an intact carbon film, attention has to be paid to avoid wetting the carbon film on the upper surface.
7. Many membrane protein 2D crystals support complete drying in glucose, without loss of the high-resolution order. A grid with a glucose embedded sample can usually be dried extensively, and even be loaded with a cryosample holder into the vacuum of the TEM, while still at room temperature. The grid quality can then be assessed at room temperature in the TEM, which, on most microscopes, is faster than handling a cryogrid at low temperatures. Only after verifying that the grid shows a suitable sample density and glucose thickness, the cryo-EM holder is filled with liquid nitrogen to cool the sample. (A different procedure may be required for Helium cooled instruments, which usually are cooled before sample insertion.) This sample preparation results in cryogrids that are completely free of ice contamination. Trehalose-embedded membrane proteins will in most cases still require the presence of traces of water. A grid prepared with trehalose should therefore only be blotted for approx 20 s (depending on air humidity), and then frozen by manual plunging into liquid nitrogen. Because trehalose prevents ice crystal formation, quick-freezing in ethane slush is not necessary. The grid can then be mounted into a pre-cooled cryo sample holder and transferred into the TEM.
8. The second piece of carbon film should be slightly smaller than the grid. To yield a symmetrical carbon film sandwich, this second carbon film should be from the same evaporation process as the first. The symmetrical carbon is essential to reduce the beam-induced specimen drift (Y. Fujiyoshi, personal communication, 2004, and Glaeser and Downing ***[33]***).

References

1. Nogales, E., Wolf, S. G., and Downing, K. H. (1998) Structure of the alpha beta tubulin dimer by electron crystallography. *Nature (London)* **391,** 199–203.
2. Henderson, R., Baldwin, J. M., Ceska, T. A., Zemlin, F., Beckmann, E., and Downing, K. H. (1990) Model for the structure of Bacteriorhodopsin based on high-resolution electron cryo-microscopy. *J. Mol. Biol.* **213,** 899–929.
3. Kühlbrandt, W., Wang, D. N., and Fujiyoshi, Y. (1994) Atomic model of plant light-harvesting complex by electron crystallography. *Nature (London)* **367,** 614–621.
4. Murata, K., Mitsuoka, K., Hirai, T., et al. (2000) Structural determinants of water permeation through aquaporin-1. *Nature (London)* **407,** 599–605.
5. Ren, G., Reddy, V. S., Cheng, A., Melnyk, P., and Mitra, A. K. (2001) Visualization of a water-selective pore by electron crystallography in vitreous ice. *Proc. Natl. Acad. Sci. USA* **98,** 1398–1403.

6. Vonck, J., von Nidda, T. K., Meier, T., et al. (2002) Molecular architecture of the undecameric rotor of a bacterial Na+-ATP synthase. *J. Mol. Biol.* **321,** 307–316.
7. Miyazawa, A., Fujiyoshi, Y., and Unwin, N. (2003) Structure and gating mechanism of the acetylcholine receptor pore. *Nature (London)* **424,** 949–955.
8. Gonen, T., Sliz, P., Kistler, J., Cheng, Y., and Walz, T. (2004) Aquaporin-0 membrane junctions reveal the structure of a closed water pore. *Nature (London)* **429,** 193–197.
9. Hirai, T., Heymann, J. A., Shi, D., Sarker, R., Maloney, P. C., and Subramaniam, S. (2002) Three-dimensional structure of a bacterial oxalate transporter. *Nat. Struct. Biol.* **9,** 597–600.
10. Grigorieff, N., Ceska, T. A., Downing, K. H., Baldwin, J. M., and Henderson, R. (1996) Electron-crystallographic refinement of the structure of bacteriorhodopsin. *J. Mol. Biol.* **259,** 393–421.
11. Mitsuoka, K., Hirai, T., Murata, K., Miyazawa, A., Kidera, A., Kimura, Y., and Fujiyoshi, Y. (1999) The structure of bacteriorhodopsin at 3.0 Å resolution based on electron crystallography: implication of the charge distribution. *J. Mol. Biol.* **286,** 861–882.
12. Fujiyoshi, Y., Mizusaki, T., Morikawa, K., et al. (1991) Development of a superfluid helium stage for high-resolution electron microscopy. *Ultramicroscopy* **38,** 241–251.
13. Downing, K. H. and Li, H. (2001) Accurate recording and measurement of electron diffraction data in structural and difference Fourier studies of proteins. *Microsc. Microanal.* **7,** 407–417.
14. Glaeser, R. M. (1992) Specimen flatness of thin crystalline arrays: influence of the substrate. *Ultramicroscopy* **46,** 33–43.
15. Gyobu, N., Tani, K., Hiroaki, Y., Kamegawa, A., Mitsuoka, K., and Fujiyoshi, Y. (2004) Improved specimen preparation for cryo-electron microscopy using a symmetric carbon sandwich technique. *J. Struct. Biol.* **146,** 325–333.
16. Vonck, J. (2000) Parameters affecting specimen flatness of two-dimensional crystals for electron crystallography. *Ultramicroscopy* **85,** 123–129.
17. Downing, K. H. (1991) Spot-scan imaging in transmission electron microscopy. *Science* **251,** 53–59.
18. Remigy, H. W., Caujolle-Bert, D., Suda, K., Schenk, A., Chami, M., and Engel, A. (2003) Membrane protein reconstitution and crystallization by controlled dilution. *FEBS Lett.* **555,** 160–169.
19. Jap, B. K., Zulauf, M., Scheybani, T., Hefti, A., Baumeister, W., Aebi, U., and Engel, A. (1992) 2D crystallization: from art to science. *Ultramicroscopy* **46,** 45–84.
20. Levy, D., Chami, M., and Rigaud, J. L. (2001) Two-dimensional crystallization of membrane proteins: the lipid layer strategy. *FEBS Lett.* **504,** 187–193.
21. Kühlbrandt, W. (1992) Two-dimensional crystallization of membrane proteins. *Q. Rev. Biophys.* **25,** 1–49.
22. Hasler, L., Heymann, J. B., Engel, A., Kistler, J., and Walz, T. (1998) 2D crystallization of membrane proteins: rationales and examples. *J. Struct. Biol.* **121,** 162–171.

23. Henderson, R. (1992) Image contrast in high-resolution electron microscopy of biological macromolecules: TMV in ice. *Ultramicroscopy* **46,** 1–18.
24. Kimura, Y., Vassylyev, D. G., Miyazawa, A., et al. (1997) Surface of bacteriorhodopsin revealed by high-resolution electron crystallography. *Nature (London)* **389,** 206–211.
25. Golas, M. M., Sander, B., Will, C. L., Lührmann, R., and Stark, H. (2003) Molecular architecture of the multiprotein splicing factor SF3b. *Science* **300,** 980–984.
26. Golas, M. M., Sander, B., Will, C. L., Lührmann, R., and Stark, H. (2005) Major conformational change in the complex SF3b upon integration into the spliceosomal U11/U12 di-snRNP as revealed by electron cryomicroscopy. *Mol. Cell.* **17,** 869–883.
27. Sander, B., Golas, M. M., and Stark, H. (2005) Advantages of CCD detectors for de novo three-dimensional structure determination in single-particle electron microscopy. *J. Struct. Biol.* **151,** 92–105.
28. Aebi, U., Smith, P. R., Dubochet, J., Henry, C., and Kellenberger, E. (1973) A study of the structure of the T-layer of *Bacillus brevis*. *J. Supramol. Struct.* **1,** 498–522.
29. Schenk, A. D., Werten, P. J., Scheuring, S., et al. (2005) The 4.5 Å structure of human AQP2. *J. Mol. Biol.* **350,** 278–289.
30. Walz, T. and Grigorieff, N. (1998) Electron crystallography of two-dimensional crystals of membrane proteins. *J. Struct. Biol.* **121,** 142–161.
31. Iancu, C. V., Wright, E. R., Heymann, J. B., and Jensen, G. J. (2006) A comparison of liquid nitrogen and liquid helium as potential cryogens for electron cryotomography. *J. Struct. Biol.* **153,** 231–240.
32. Comolli, L. R. and Downing, K. H. (2005) Dose tolerance at helium and nitrogen temperatures for whole cell electron tomography. *J. Struct. Biol.* **152,** 149–156.
33. Fujiyoshi, Y. (1998) The structural study of membrane proteins by electron crystallography. *Adv. Biophys.* **35,** 25–80.
34. Glaeser, R. M. and Downing, K. H. (2004) Specimen charging on thin films with one conducting layer: Discussion of physical principles. *Microsc. Microanal.* **10,** 790–796.
35. Butt, H.-J., Wang, D. N., Hansma, P. K., and Kühlbrandt, W. (1991) Effect of surface roughness of carbon support films on high-resolution electron diffraction of two-dimensional protein crystals. *Ultramicroscopy* **36,** 307–318.
36. Booy, F. P. and Pawley, J. B. (1993) Cryo-crinkling: what happens to carbon films on copper grids at low temperature. *Ultramicroscopy* **48,** 273–280.
37. Mindell, J. A., Maduke, M., Miller, C., and Grigorieff, N. (2001) Projection structure of a ClC-type chloride channel at 6.5 Å resolution. *Nature (London)* **409,** 219–223.